

# Short Pulse Propagation along Microstrip Meander Delay Lines with Design Constraints: Comparative Analysis of the Quasi-static and Electromagnetic Approaches

Pavel Orlov, Talgat Gazizov, and Aleksander Zabolotsky

Department of Television and Control  
Tomsk State University of Control Systems and Radioelectronics, Tomsk, 634050, Russia  
praetorian281@gmail.com, talgat@tu.tusur.ru, zabolotsky\_am@mail.ru

**Abstract** — Short pulse propagation along microstrip meander delay lines is considered. Electromagnetic analysis is used in the CST MWS software. A quasi-static analysis in TALGAT software is used as another approach, for which the complete computational models for capacitive matrix calculation are presented. The results of simulations are given. It is shown that if a number of turns is increased and their length is reduced proportionally, distortions of a pulse signal in the line are reduced. At the same time, though the electrical width of the structure increases, an agreement between the results of quasi-static and electromagnetic analyses is improved. Memory costs of electromagnetic analysis and quasi-static analysis are comparable, while the latter is significantly less time-consuming. Thus, it is demonstrated that a quasi-static analysis can be quite relevant during the design of the microstrip meander delay lines with minimal distortions.

**Index Terms** — Electromagnetic analysis, meander delay line, quasi-static approach.

## I. INTRODUCTION

Trends of modern electronics devices development (decrease in dimensions, increase in the upper frequency of signal spectrum, etc.) lead to increase in package density and to the need for signals asynchrony minimization. In this regard, delay lines, particularly in the form of a meander, as the simplest structure, are widely used. However, crosstalk arises, and it can distort waveform and reduce delay time of a pulse propagating in the line [1]. There are different approaches to crosstalk level reduction, for example, use of guard traces [2], but it increases the area of meander lines. Meanwhile, it is often required to minimize the area of meander lines.

These factors lead to the need for numerical analysis of meander lines. Two approaches to the analysis are used: quasi-static and electromagnetic. The first approach is usually less consumptive but it is an approximation, as it is based on the telegraph equations,

which are valid only for small electrical width of a structure. The second approach takes into account higher order modes but is more consumptive and requires more user's competencies [3] than the work with the quasi-static approach.

Electromagnetic analysis for a one set of parameters of the microstrip meander delay line is presented in [4]. A similar analysis, but in the range of parameters, is made in [5]. Comparison between the electromagnetic and quasi-static analysis results and the experimental results obtained for the strip line is given in [6]. Comparison of the results obtained by three different numerical methods for one set of microstrip line parameters is presented in [7]. These studies did not investigate applicability of the quasi-static analysis for the case of electrically wide structures, in particular, when delay time and area of the meander microstrip line are defined and it is necessary to minimize distortions of the pulse signal. Meanwhile, such a research is very important for design process because it will help to optimize both parameters and analysis process of the meander delay lines. The aim of this paper is to compare the results of electromagnetic and quasi-static simulations of a short pulse propagation along microstrip meander delay lines with design constraints.

## II. SIMULATION APPROACHES

In this paper simulation of the meander lines was executed in the CST MWS and TALGAT software without accounting the losses in conductors and dielectrics.

In CST MWS a combination of the perfect boundary approximation with the Finite Integration Technique is used [8]. The transient solver allows to make full-wave 3D analysis of structures of various complexities. In general, the system is widely known to give it a more detailed description. In order to demonstrate that quasi-static approach can be useful for simulation of meander lines, TALGAT software is used. Let us give a more detailed description of the features of quasi-static

approach implemented in TALGAT software.

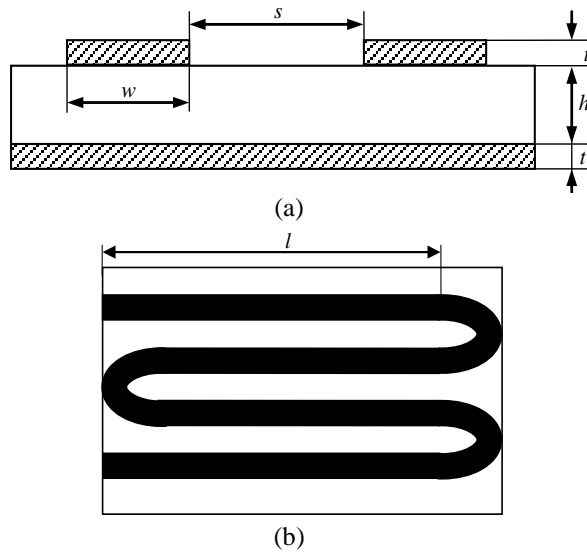


Fig. 1. Cross section of a turn model (a) and top view of two turns (b).

The TALGAT software is based on the method of moments and allows to make 2D quasi-static analysis. The algorithm implemented in the system allows to calculate all elements of a moment matrix by fully analytical formulae only, avoiding the time-consuming and approximate numerical integration. It can be useful for effective calculation of a capacitive matrix of two-dimensional systems of various complexities [9]. In this paper the simulation of the short pulse propagation in meander lines is carried out. A multiconductor transmission line is a base of the considered structures. It is assumed in the analysis that a transmission line is uniform along its length with an arbitrary cross section. The cross section, in general case, with  $N$  signal conductors and a reference, is represented by the following  $N \times N$  matrices of line per unit length parameters: inductance ( $\mathbf{L}$ ), coefficients of electrostatic induction ( $\mathbf{C}$ ), resistance ( $\mathbf{R}$ ), conductance ( $\mathbf{G}$ ). In paper [10], an approach based on a modified nodal admittance matrix has been presented for formulation of network equations including the coupled transmission line, terminal, and interconnecting networks. The approach is used and voltages in the time domain are obtained by applying the inverse fast Fourier transform. Matrixes  $\mathbf{L}$  and  $\mathbf{C}$  are calculated by a method of moments and the mathematical model for considered case of linear and orthogonal boundaries of conductors and dielectrics [11] implemented in TALGAT system is described below.

First we are segmenting the conductor-dielectric boundaries (subdividing them into intervals further called subintervals) and assign numbers from 1 to  $Nc$  to these subintervals. Then we digitize the dielectric-

dielectric boundaries and assign them numbers from  $Nc + 1$  to  $N$ . (The infinite ground plane is not digitized. If there is a second infinite plane, it is bounded at a point far removed from the conductors, digitized as a conventional conductor, and considered to be at zero potential. If there are other conductors that are always at zero potential, they all are conventionally digitized.) In so doing, we first digitize and number the conductor-dielectric subintervals orthogonal to the  $Y$  axis (the serial number of the last subinterval is  $Nc_Y$ ), digitize and number the conductor-dielectric subintervals orthogonal to the  $X$  axis (the serial number of the last subinterval is  $Nc$ ), digitize and number the dielectric-dielectric subintervals orthogonal to the  $Y$  axis (the serial number of the last subinterval is  $Nd_Y$ ), and finally digitize and number the dielectric-dielectric subintervals orthogonal to the  $X$  axis (the serial number of the last subinterval is  $N$ ).

Each subinterval has the following parameters: the coordinate of the  $X$ -center of the  $n$ th subinterval is  $x_n$ , the coordinate of the  $Y$ -center of the  $n$ th subinterval is  $y_n$ , the length of the  $n$ th subinterval is  $d_n$ ; the permittivity of the  $n$ th conductor-dielectric subinterval is  $\varepsilon_n$ , and the permittivities on the positive (to which the vector  $\mathbf{n}_n$  is pointed) and negative sides (from which the vector  $\mathbf{n}_n$  is emanated) of the  $n$ th dielectric-dielectric subinterval are  $\varepsilon_n^+$  and  $\varepsilon_n^-$ , respectively. Here  $\mathbf{n}_n$  is a unit normal vector drawn from the center of the  $n$ th subinterval. These parameters are used to calculate the entries of matrix of linear system to be solved.

For the matrix rows with numbers  $m = 1, \dots, Nc$  we have:

$$S_{mm} = \frac{1}{2\pi\varepsilon_0} (\hat{I}_{mm} - I_{mm}), \quad \begin{cases} m=1, \dots, Nc \\ n=1, \dots, N \end{cases}$$

Here for  $n = 1, \dots, Nc_Y, (Nc + 1), \dots, Nd_Y$  we have:

$$I_{mm} = a_1 \cdot \ln(a_1^2 + c_1^2) - 2a_1 + 2c_1 \cdot \arctg\left(\frac{a_1}{c_1}\right) - a_2 \cdot \ln(a_2^2 + c_1^2) + 2a_2 - 2c_1 \cdot \arctg\left(\frac{a_2}{c_1}\right), \quad (1)$$

where

$$a_1 = \frac{d_n}{2} - (x_m - x_n); \quad a_2 = \frac{-d_n}{2} - (x_m - x_n); \quad c_1 = y_m - y_n. \quad (2)$$

$\hat{I}_{mm}$  is calculated from Eq. (1) in which  $c_1$  is substituted by  $c_2$ . Then we obtain:

$$a_1 = \frac{d_n}{2} - (x_m - x_n); \quad a_2 = \frac{-d_n}{2} - (x_m - x_n); \quad c_1 = y_m - y_n. \quad (3)$$

For  $n = (Nc_Y + 1), \dots, Nc, (Nd_Y + 1), \dots, N$ ,  $I_{mm}$  is calculated from Eq. (1) and,

$$a_1 = \frac{d_n}{2} - (y_m - y_n); \quad a_2 = \frac{-d_n}{2} - (y_m - y_n); \quad c_1 = x_m - x_n. \quad (4)$$

$\hat{I}_{mn}$  is calculated from Eq. (1) in which  $c_1$  is replaced by  $c_2$ :

$$a_1 = \frac{d_n}{2} + (y_m + y_n); a_2 = \frac{-d_n}{2} + (y_m + y_n); c_2 = x_m - x_n. \quad (5)$$

For the matrix rows with numbers  $m = (Nc + 1), \dots, N$ , we have:

$$S_{mn} = \frac{1}{2\pi\epsilon_0} (I_{mn} - \hat{I}_{mn}), \begin{cases} m=(Nc+1), \dots, N \\ n=1, \dots, N \end{cases}, m \neq n;$$

$$S_{mn} = \frac{1}{2\pi\epsilon_0} (I_{mn} - \hat{I}_{mn}) + \frac{1}{2\epsilon_0} \frac{\epsilon_m^+ + \epsilon_m^-}{\epsilon_m^+ - \epsilon_m^-}, m=(Nc+1), \dots, N,$$

where for the rows with numbers  $m = (Nc + 1), \dots, Nd_Y$  for  $n = 1, \dots, Nc_Y, (Nc + 1), \dots, Nd_Y$ ,

$$I_{mn} = \arctg\left(\frac{a_1}{c_1}\right) - \arctg\left(\frac{a_2}{c_1}\right), \quad (6)$$

and the variables coincide with those defined by Eq. (2);  $\hat{I}_{mn}$  is calculated from Eq. (6) after replacement of  $c_1$  by  $c_2$  and substitution of Eq. (3), and for  $n = (Nc_Y + 1), \dots, Nc, (Nd_Y + 1), \dots, N$ , we have:

$$I_{mn} = \frac{1}{2} \ln\left(\frac{a_2^2 + c_1^2}{a_1^2 + c_1^2}\right), \quad (7)$$

where the variables coincide with those defined by Eq. (4), and  $\hat{I}_{mn}$  is calculated from Eq. (7) taken with opposite sign after replacement of  $c_1$  by  $c_2$  and substitution of Eq. (5). For the matrix rows with numbers  $m = (Nd_Y + 1), \dots, N$  for  $n = 1, \dots, Nc_Y, (Nc + 1), \dots, Nd_Y$ ,  $I_{mn}$  is calculated from Eq. (7) with variables defined by Eq. (2), and  $\hat{I}_{mn}$  is calculated from Eq. (7) after replacement of  $c_1$  by  $c_2$  and substitution of Eq. (3). For  $n = (Nc_Y + 1), \dots, Nc, (Nd_Y + 1), \dots, N$ ,  $I_{mn}$  is calculated from Eq. (6) with the variables coinciding with those defined by Eq. (4), and  $\hat{I}_{mn}$  is calculated from Eq. (6) after replacement of  $c_1$  by  $c_2$  and substitution of Eq. (5).

Now the linear system to be solved assumes the form:

$$\sum_{n=1}^N S_{mn} \sigma_n = \begin{cases} V_i, & m=1, \dots, Nc, \\ 0, & m=(Nc+1), \dots, N \end{cases}.$$

The subscript  $i$  here means that each digitized element belonging to the  $i$ th conductor is at the potential required for the determination of the capacitance matrix. The components  $S_{mn}$  gathered together yield the quadratic matrix  $\mathbf{S}$  relating the charge densities of segmented elements on the conductors and the dielectric boundaries, forming the vector  $\boldsymbol{\sigma}$ , with the potentials of these elements forming the vector  $\mathbf{V}$ , and the problem itself is expressed in the compact linear system form  $\mathbf{S}\boldsymbol{\sigma} = \mathbf{V}$ , which is solved  $N_{cond}$  times (where  $N_{cond}$  is

the number of conductors in the system disregarding the reference conductor), and in the  $i$ th solution, the conductor potential  $V_i, i = 1, \dots, N_{cond}$ , is set equal to 1 V, and the potentials of all remaining conductors are set equal to 0 V. Finally, from the definition of the entry of the capacitance matrix we obtain:

$$C_{ij} = \sum_{n=NF_i}^{NL_i} \frac{\epsilon_n}{\epsilon_0} \sigma_n^{(j)} d_n, i, j = 1, \dots, N_{cond}.$$

Here,  $NF_i$  and  $NL_i$  are the numbers of the first and last subintervals of the  $i$ th conductor, the subscript  $i$  denotes the conductor for which charges  $\sigma_n^{(j)}$  are summed, and the superscript  $j$  indicates the serial number of  $\sigma_n$  calculated when the potential of the  $j$ th conductor is set equal to 1 V and the potentials of the remaining conductors are set equal to 0 V.

### III. SIMULATION RESULTS

In the TALGAT system the meander line structure was represented like  $N$ -conductor transmission line, with ends of the conductors connected respectively (see Fig. 2). Structures with  $N = 2; 4; 8; 16; 32$ , with the length ( $l$ ) of 20; 10; 5; 2.5; 1.25 mm were selected respectively. It allows to get electrically narrow and wide structures with a constant total length of conductors. The cross section of the analyzed structure is shown in Fig. 1 (a). Its parameters are: conductors thickness ( $t$ ) – 35  $\mu\text{m}$ , conductors width ( $w$ ) – 50  $\mu\text{m}$ , distance between conductors ( $s$ ) – 50  $\mu\text{m}$ , dielectric material ( $\epsilon_r = 3.8$ ; thickness ( $h$ ) – 2 mm). These parameters were chosen in such a way that a high level of electromagnetic coupling is generated between the half-turns, which maximizes the pulse distortions. The value of the resistance at the ends of the line was chosen under pseudomatching conditions as 205  $\Omega$ . A trapezoidal signal with EMF 1 V and duration of rise and fall – 0.1 ns, flat top – 1 ns was chosen as the excitation source. Memory costs and computational costs are given in Table 1. Waveforms at the output of the meander line are shown in Fig. 3. Signal propagation delays at "0.5" level are given in Table 2.

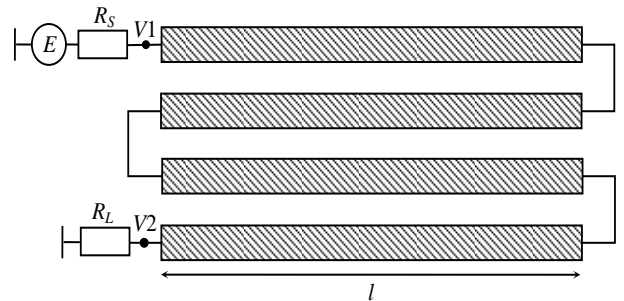


Fig. 2. Circuit diagram of a meander line model for quasi-static simulation with  $N = 4$ .

Table 1: The consumption of computer memory and CPU time for CST MWS and TALGAT

$N$	CST MWS		TALGAT	
	Time, sec	Peak Memory Usage, Mb	Time, sec	Peak Memory Usage, Mb
2	1002	345	3	85
4	822	306	6.2	107
8	730	288	17.3	185
16	635	263	60	586
32	796	303	62	501

Table 2: Comparison of delay times at level «0.5» from Fig. 3

$N$	$l$ , mm	$T_{CST}$ , ps	$T_{TALGAT}$ , ps	$\Delta T$ , ps	$\frac{ T_{CST} - T_{TALGAT} }{T_{CST} + T_{TALGAT}} \cdot 100\%$
2	20	87	206	119	40
4	10	105	129	24	10
8	5	93	109	16	8
16	2.5	90	100	10	5
32	1.25	89	104	15	8

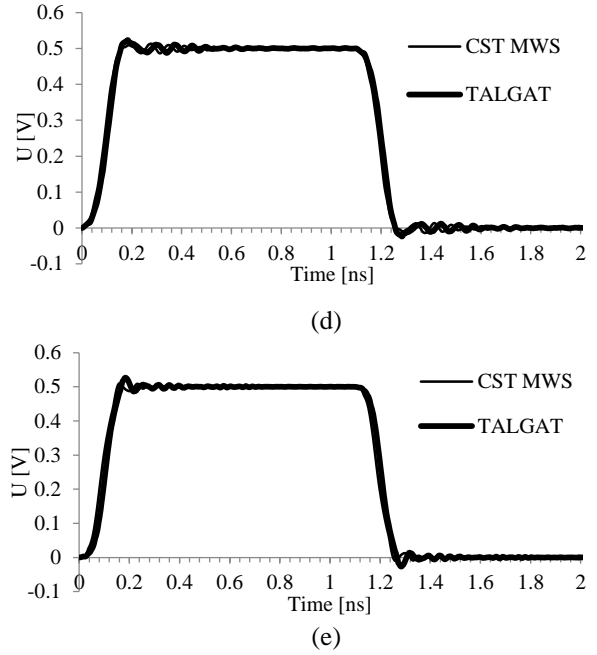
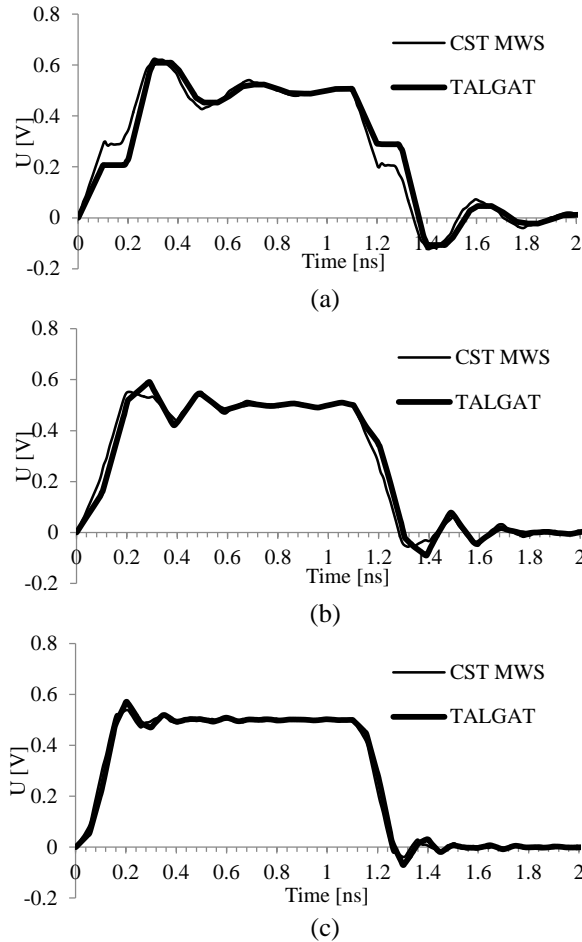


Fig. 3. Output waveforms of the examined structures with  $N = 2$  (a); 4 (b); 8 (c); 16 (d); and 32 (e).

From these results it is clear that the waveform of the signal is subjected to distortions caused by electromagnetic coupling between the half-turns. However, the results of quasi-static and electromagnetic analysis showed good agreement: delays difference does not exceed 10%, and only in case of  $N = 2$  it equals to 40% due to the difference of the near end crosstalk levels, that may be caused by neglect of edge effects at the ends of the halfturns in quasi-static analysis. Reduction of pulse distortion, obtained through the increase of  $N$  and corresponding reduction of half-turn length, can be explained by the reduction of propagation delay in a single turn and, consequently, reduction of delay between the signal and the near end crosstalk. It leads to the reduction of distortions at the rise and fall of a pulse, which are significant for  $N = 2$  only. As far as the difference between the results of electromagnetic and quasi-static analyses is most obviously observed in difference of their amplitudes of the near end crosstalk (which is clearly seen in Fig. 3 (a)), the increase of  $N$  and the corresponding decrease of the turn length provide more coincident results.

For the upper frequency of signal spectrum (10 GHz) the wavelength in vacuum equals to 3 cm and with the dielectric it is somewhat smaller. When  $N = 32$ , structure width (3.25 mm) is more than  $0.1\lambda$ , which can lead to incorrect results of quasi-static analysis. However, we observe the overall coincidence of quasi-

static and electromagnetic analysis results that allows us to conclude the correctness of the quasi-static analysis for structures of this type. For the considered cases, memory costs of CST MWS and TALGAT are comparable, while TALGAT is 12–334 times less time-consuming.

#### IV. CONCLUSION

The complete computational models for capacitive matrix calculation of quasi-static approach are presented. In spite of the considered simplicity and limitations of the quasi-static approach, it can give accurate, on a par with electromagnetic approaches, and fast results even for structures with complex electromagnetic coupling. It is worth noting, though the electrical width of a structure increases, the agreement between the results of quasi-static and electromagnetic analyses is improved. Thus, it is demonstrated that a quasi-static analysis can be quite relevant during the design of microstrip meander delay lines with minimal distortions. This is especially important at the stage of optimization that requires repetitive calculations.

Results of simulation allow to conclude that the larger number of turns gives smaller waveform distortions for structures with the same total length of lines.

#### ACKNOWLEDGMENT

Authors thank reviewers for valuable comments. Development of necessary software was supported by the state contract 8.1802.2014/K of the Russian Ministry of Education and Science, modeling of coupled lines was supported by RFBR grant 14-29-09254, simulation of waveforms was carried out at the expense of RSF grant 14-19-01232 in TUSUR University.

#### REFERENCES

- [1] R. B. Wu and F. L. Chao, "Laddering wave in serpentine delay line," *IEEE Trans. Compon., Packag., Manuf. Technol.*, vol. 18, no. 4, pt. B, pp. 644-650, Nov. 1995.
- [2] S. Guang-Hwa, C. Chia-Ying, and R. B. Wu, "Guard trace design for improvement on transient waveforms and eye diagrams of serpentine delay lines," *IEEE Transactions on Advanced Packaging*, vol. 33, no. 4, p. 1051-1060, 2010.
- [3] A. Bruce, "Importance and process of validation for all levels of modeling problems," *Proc. of the 2009 IEEE Int. Symp. on EMC*, 2009.
- [4] E. Topsakal and J. Volakis, "Finite element method for the accurate analysis of delay line propagation characteristics," *IEEE International Symposium on EMC*, vol. 2, pp. 1074-1076, 2003.
- [5] A. Kabiri, Q. He, M. H. Kermani, and O. M. Ramahi, "Design of a controllable delay line," *IEEE Transactions on Advanced Packaging*, vol. 33, no. 4, pp. 1080-1087, 2010.
- [6] B. J. Rubin and B. Singh, "Study of meander line delay in circuit boards," *IEEE Transactions on Microwave Theory and Techniques*, vol. 48, no. 9, pp. 1452-1460, 2000.
- [7] A. U Bhohe, C. L. Holloway, and M. Picket-May, "Meander delay line challenge problem: a comparison using FDTD, FEM and MoM," *IEEE International Symposium on EMC*, vol. 2, pp. 805-810, 2001.
- [8] *The Finite Integration Technique*, [Online]. Available: <https://www.cst.com/Products/CSTMws/FIT>
- [9] T. R. Gazizov, "Analytic expressions for Mom calculation of capacitance matrix of two dimensional system of conductors and dielectrics having arbitrary oriented boundaries," *Proc. of the 2001 IEEE EMC Symposium, Montreal, Canada*, vol. 1. pp. 151-155, Aug. 13-17, 2001.
- [10] J. R. Griffith and M. S. Nakhla, "Time-domain analysis of lossy coupled transmission lines," *IEEE Transactions on Microwave Theory and Techniques*, vol. 38, pp. 1480-1487, 1990.
- [11] T. R. Gazizov, "Calculation of a capacitance matrix for a two-dimensional configuration of conductors and dielectrics with orthogonal boundaries," *Russian Physics Journal*, vol. 47, pp. 326-328, 2004.



**Orlov Pavel Evgenievich** was born in 1986. He received the Ph.D. degree from Tomsk State University of Control Systems and Radioelectronics, Tomsk Region, Russia in 2013. His research interest is electromagnetic compatibility. Evgenievich is the author of 47 scientific papers.



**Gazizov Talgat Rashitovich** was born in 1963. He got his higher professional education on Radioengineering in 1985 in the Tomsk Institute of Automatic Control Systems and Radioelectronics, Ph.D degree in 1999, and Doctor of Sciences degree in 2010. His research interest is electromagnetic compatibility. He is author of 242 scientific publications.



**Zabolotsky Alexander Mikhailovich**

was born in 1982. He got his higher professional education on Radioengineering in 2004 in the Tomsk State University of Control Systems and Radioelectronics, Ph.D. degree in 2010. His research interest is electromagnetic compatibility. He is author of 160 scientific publications.